# Dynamical Climatology

## A scheme for incorporating the thermodynamic sea-ice model into a coupled ocean-atmosphere model.

by

C. Gordon and M. Bottomley

DCTN 1 June 1984

Meteorological Office (Met. O. 20)
London Road
Bracknell
Berkshire RG12 2SZ

JB/16

DYNAMICAL CLIMATOLOGY TECHNICAL NOTE NO. 1

# A SCHEME FOR INCORPORATING THE THERMODYNAMIC SEA-ICE MODEL INTO A COUPLED OCEAN-ATMOSPHERE MODEL

by

C GORDON AND M BOTTOMLEY

Met O 20 (Dynamical
Climatology Branch)
Meteorological Office
London Road
Bracknell
Berkshire RG12 2SZ

June 1984

Note: This paper has not been published. Permission to quote from it should be obtained from the Assistant Director of the above Meteorological Office Branch.

## 1. Introduction

The ocean/atmosphere coupled model which is currently under development in Met O 20 will contain a simple representation of sea-ice growth and decay due to thermodynamic processes. Ice will form in the model when the ocean surface temperature drops below freezing and then grow or decay according to the net heat budget of the ice block. Open water appears when the ice depth falls to zero.

A diurnal cycle of radiative heating is explicitly represented in the atmospheric model and surface exchanges of heat and moisture are calculated every timestep(e.g. 10-20 minutes). It is also desirable to update the sea-ice surface temperature every timestep. This is because the non-linearity of the outgoing infra-red flux may lead to significant errors in the surface heat balance if the diurnal variation of temperature is not included. The diurnal cycle of day-time melting and night-time freezing also affects the short wave radiative budget at the surface as a consequence of the changing surface albedo. Over the open ocean, however, there is little justification for including the diurnal cycle of sea-surface temperature explicitly. This is especially true in a model with a globally constant mixed layer depth since the heat capacity of this layer is sufficiently large that it would make no significant difference.

Typically the ocean surface temperature will be updated on the timescale of days whereas the ice surface temperature will be updated much more frequently.

Figure 1 indicates a typical mode of coupling in a synchronous ocean/atmosphere experiment. The atmospheric model would run for N days (where N is likely to be of order 1 to 5) during which the heat and

momentum fluxes required by the ocean model would be accumulated. At the end of this N day period the ocean model would be called and the sea-surface temperature updated and passed back to the AGCM for use over the next N days. The value of N is determined by computational and physical considerations. The computational factor is that if it is necessary to swap the ocean and atmosphere models in and out of the computer main memory, it is clearly desirable to make N as large as possible so as to minimise the time spent in the programme interchange. However, if both models fit in core, this is not a limitation. The physical considerations concern the extent to which N determines the frequency spectrum of forcing passed across to the ocean model. It is not desirable to resolve short timescale dynamical motions in the ocean model if their dissipation mechanisms are not adequately parameterised, so that to choose N as small as possible is not necessarily the best option.

Incorporating the sea-ice model into the scheme illustrated in Figure 1 can lead to problems because of the explicit representation of the diurnal cycle in ice surface temperature. Complications occur when a sea-ice point changes to a sea point part way through the N-day cycle. Although these can be overcome, the coding required is rather cumbersome and a much simpler scheme is to update the ice surface temperature every atmospheric model timestep but to update the ice depth only every N days. In this way the classification of a point can only change in the oceanic leg of the cycle.

In the sections below the physical applicability of such a 'dual timestep' scheme will be discussed and the modifications to the basic model to include the diurnal cycle and snow cover will be looked at in

detail.

## 2. Basic Equations

In this section the fundamental equations which are common to all thermodynamic sea-ice models will be written down and discussed. Snow cover will be included in a later section.

Consider the coordinates $h_1$, and $h_2$ as defined in Figure 2. These are the coordinate distances of the upper and lower ice surfaces respectively. They are introduced so that latent heat changes can be expressed separately at each boundary. The temperature profile inside the ice block will satisfy the diffusion equation:

$$c\rho \frac{\partial T}{\partial t} = \frac{\partial}{\partial z}\left(\kappa \frac{\partial T}{\partial z}\right) \tag{2.1}$$

The symbols used throughout this note are defined in Appendix A. If the penetration of short wave radiation is included an additional flux divergence term appears in (2.1).

The boundary conditions on (2.1) depend on whether there is surface melting. If there is no surface melting, then

$$-\kappa \frac{\partial T}{\partial z}\bigg|_{z=h_1} = -R_w + R_{LD} + (1-\alpha)R_S - H_S - H_L \tag{2.2}$$

$$-\kappa \frac{\partial T}{\partial z}\bigg|_{z=h_2} = -F_B - q_1 \frac{dh_2}{dt} \tag{2.3}$$

$$T(h_2,t) = T_B \quad . \tag{2.4}$$

Equation (2.2) expresses the balance between the net surface heating and the diffusive heat flux at the surface. Since there is no surface melting $h_1$ does not change and there is no latent heat term in the equation. Equation (2.3) expresses the balance between the bottom oceanic heat flux, $F_B$, the bottom diffusive heat flux and the latent heat term due to melting or freezing at the ice bottom. Finally, (2.4) ensures that the temperature at the ice bottom remains fixed at the freezing point of sea water. ($T_B$ = 271.2K).

If there is surface melting the appropriate boundary conditions are

$$-\kappa \frac{\partial T}{\partial z}\bigg|_{z=h_1} = -R_{LU} + R_{LD} + (1-\alpha)R_S - H_S - H_L - q\frac{dh_1}{dt} \tag{2.5}$$

$$-\kappa \frac{\partial T}{\partial z}\bigg|_{z=h_2} = -F_B - q\frac{dh_2}{dt} \tag{2.6}$$

$$T(h_2,t) = T_B \tag{2.7}$$

$$T(h_1,t) = T_o \quad . \tag{2.8}$$

Since there is surface melting the upper coordinate $h_1$ now enters as a prognostic variable. The last term in (2.5) is the latent heat flux due to this melting. Equation (2.8) expresses the fact that the surface temperature remains fixed at the melting point, $T_o$, when melting

occurs. Because of the residual salinity in the ice $T_o$ is assumed to be 273.05K (Maykut and Untersteiner, 1971). (Note that $T_B$ is less than $T_o$ because of the higher salinity of the newly formed ice at the lower boundary).

Any model of sea-ice must match together the regimes of melting and freezing discussed above to produce a continuous solution for the ice temperature profile and ice depth. (The ice depth $h = h_2 - h_1$).

It may be noted here that the mass balance of the snow-ice system is also affected by sublimation and, during melting, by evaporation. For consistency with previous work (Maykut and Untersteiner, 1971; Semtner, 1976; Bottomley, 1984) these effects were not included in the initial tests of the dual timestep scheme reported here. They will however be included when the scheme is incorporated into the coupled atmosphere-ocean model.

In general, each of the physical parameters $c, \rho, k$ and $q$ will be a function of temperature and salinity and therefore, functions of depth. Thermodynamic ice models differ in the detail with which the non-uniformity of the physical parameters are represented, as well as in the numerical scheme used to solve for the temperature profile. In what follows all of these parameters will be assumed constant.

It will be useful to rearrange the above equations slightly. Consider the heat budget of the whole ice block by integrating the diffusion equation (2.1) over the block. This gives

$$\frac{dH}{dt} = k \left.\frac{\partial T}{\partial z}\right|_{z=h_2} - k \left.\frac{\partial T}{\partial z}\right|_{z=h_1} \qquad (2.9)$$

which, on using (2.2) and (2.3) or (2.5) and (2.6), gives,

$$\frac{dH}{dt} = -R_{LU} + R_{LD} + (1-\alpha)R_S - H_S - H_L + F_B + \rho_I \frac{dh}{dt} \qquad (2.10)$$

where $H$ is the heat content of the ice block and $h$ is the ice thickness. Equation (2.10) illustrates that the change in heat content of the ice block is equal to the heat input minus the latent heat used in melting. Equation (2.10) may be integrated to give an equation for the time evolution of the ice depth. This is

$$h(t) = h(t_0) - \frac{1}{\rho_I}\int_{t_0}^{t}\{-R_{LU} + R_{LD} + (1-\alpha)R_S - H_S - H_L + F_B\}dt + H(t) - H(t_0) \qquad (2.11)$$

Note that the surface fluxes are dependent on the surface temperature and that this temperature depends upon the ice depth. Despite its apparently simple form, (2.11) is actually a highly non-linear equation.

The atmospheric heating terms in the surface balance equation provide forcing on many different timescales. The ice surface temperature will also respond on these multiple timescales but the response of the ice depth will depend on the importance of the heat storage term in (2.10). It will be convenient to discuss the ice depth response to imposed surface forcing by considering the 'surface melting' and 'no surface melting' regimes separately.

a. No surface melting

In this regime changes in ice depth occur due to melting or accretion at the ice bottom. Equation (2.3) then implies that the timescale of the response in $h_2(t)$ will be determined by the variability present in the bottom diffusive heat flux $-\kappa \frac{\partial T}{\partial z}\Big|_{z=h_2}$. It might be anticipated that for surface forcing on 'long' timescales temperature variations will be transmitted to the ice bottom since the downward diffusive heat flux in the ice block has the same sign over fairly long periods. For shorter timescales the surface temperature increases and then decreases within a short period. The diffusive heat flux in the ice therefore changes sign more frequently preventing the signal diffusing downwards.

To look at this in more detail the analytic solution for the equilibrium temperature profile in an ice block of constant thickness has been obtained. In the equations that follow $h_1$ has been taken as zero so that $h_2 = h$. The boundary conditions imposed were $T(h,t) = T_B$ and $T(0,t) = \bar{T} + \Delta T \cos(\omega t)$, where $\omega = \frac{2\pi}{\tau}$ and $\tau$ is the timescale of the surface wave. The solution of equation (2.1) has the form

$$T(z,t) = (\bar{T} - T_B)\left(1 - \frac{z}{h}\right) + A(z).\Delta T.\cos(\omega t + \phi(z)) + T_B \quad (2.12)$$

The amplitude $A(z)$ and phase $\phi(z)$ are complicated functions of $z$, $h$ and $\delta$, where $\delta = (\kappa\tau/\pi c\rho)^{1/2}$. Figure 3 shows the amplitude $A(z)$ with $h = 2m$. and for timescales with $\tau$ = 1 day (diurnal), 5 days (synoptic) and 1 year (seasonal). For diurnal and synoptic scales there is no significant temperature change in the lower half of the

ice block whereas for seasonal timescales the amplitude function is essentially linear. However, this does not imply that the temperature profile is linear because of the phase term occurring in the solution (2.12).

The phase function $\phi(z)$ is shown in Figure 4. It gives information regarding the time lag with depth of the temperature waves. The cosine function in (2.12) can be re-written as $\cos\left(\frac{2\pi}{\tau}\left(t+\frac{\tau\phi}{2\pi}\right)\right)$ so that $\frac{\tau\phi(z)}{2\pi}$ is the time lag at a depth $z$ associated with a surface temperature cycle of period $\tau$. For example, for the seasonal timescale the temperature near the ice bottom lags the surface temperature by approximately 0.2 x 365 = 73 days.

It is clear from Figure 3 that the diffusive heat flux at the lower ice interface will not show any variation over the diurnal and synoptic timescales. For the seasonal timescale, because the amplitude $A(z)$ is essentially linear, the temperature profile in (2.12) can be written as

$$T(z,t) \approx \left(\bar{T}+\Delta T.\cos(\omega t+\phi(z))-T_B\right)\left(1-\frac{z}{h}\right)+T_B \qquad (2.13)$$

The diffusive heat flux at the ice bottom is found from the vertical derivative of (2.13) evaluated at $z=h$. Over seasonal timescales it is the phase term $\phi(z)$ which introduces non-linearities into the profile.

Figure 5, which is taken from Maykut and Untersteiner (1971), shows an observed temperature profile. For much of the year the profile looks linear, indeed more so than would be expected from

the analytic solution (2.12). This is probably because a simple cosine function is not a very good representation of the seasonal variation of surface temperature in the central Arctic. The profile is most markedly non-linear during the spring heating and autumn cooling. It follows from the diffusion equation 2.1 that the heat capacity of the ice plays its most significant role when the time changes in surface temperature are a maximum. (This equation also implies that during these periods the temperature profile will be non-linear).

The analytic results and observations suggest that providing the ice is sufficiently thick (see Figure 4) there will be virtually no diurnal or synoptic signal in the latent heat changes at the lower interface. Over seasonal timescales the diffusive heat flux can be calculated to a reasonable approximation by assuming a linear temperature profile. This will, however, lead to errors during the spring and autumn. (See the discussion in Section 3 for a quantitative estimate of these errors).

b. Surface melting

Surface melting can occur on all timescales in response to the variations in surface forcing. Over the timescale of the melting season ($\sim$ 3 months), the surface temperature is effectively held fixed at the melting point. Therefore during this period a linear temperature gradient might be expected throughout the ice. However, superimposed on this climatological melting are diurnal and synoptic cycles of melting and refreezing, which establish large

temperature gradients near the surface. The variations in ice depth corresponding to these will obviously exhibit fairly short timescale variations.

## 3. The zero layer model

The assumption of a linear temperature profile in the ice block, which is equivalent to neglecting the heat capacity, has been used by a number of authors as the basis of a simple thermodynamic ice model (Bryan 1969, Semtner 1976).

In these models the temperature gradient in the ice is approximated by

$$-\kappa \frac{\partial T}{\partial z} = \frac{\kappa (T_* - T_B)}{h} \qquad (3.1)$$

In Bryan's model an additional term $h_o$ = 1.7 cm is included in the denominator in an attempt to parameterise the independence of ice growth on ice depth when the ice is very thin. (However, considering the neglect of many other important physical processes, the inclusion of this term does not really seem justified).

Semtner (1976) has compared the simulations produced with a multi-level model with those from a 'zero layer' model in which the temperature profile throughout the ice is linear and of the form (3.1). Note that from equation (2.1) this implies a zero heat capacity. Identical seasonally varying forcing was used in each model. The zero layer model produces annual mean equilibrium ice depths which are 12 per cent lower than those predicted by the multi-level model. Semtner

attributes this difference to the lack of heat storage in the zero layer model. In Semtner's zero layer model the thermal diffusivity of the ice (and snow) is increased slightly to compensate for this error.

In the interactive atmosphere/ocean/sea-ice model currently under development in Met O 20 only the growth and decay of ice due to local thermodynamic processes is being included. Ice dynamics and the parametrisation of leads will be incorporated in a later version of the model. In the current model, where the representation of these other important physical processes is omitted, there is little justification in treating the thermodynamics in any greater detail than in the zero layer model. When additional ice processes are included a multi-level model of ice thermodynamics might be more appropriate.

## 4. The diurnal cycle

The reasons for wanting to include the diurnal cycle over sea-ice have already been given in the introduction. However, the assumption of a linear temperature profile in the ice, as used in the zero layer model, is not applicable to the diurnal timescale. A typical e-folding depth for a surface induced temperature wave of diurnal frequency is about 20 cm. In other words, diurnal temperature variations are only felt in the top half-metre of the ice block. This being the case, the temperature profile can obviously not be linear over the whole block.

If the zero layer model is run with an explicit diurnal cycle the diurnal range of temperature is over-estimated. This is because the large vertical temperature gradients near the ice surface which should occur are absent. In practice this gives a large diffusive heat flux in the near surface layer, away from the surface as the surface temperature

is increasing but in the opposite direction once the temperature starts to decrease. In this way the variation in surface temperature throughout the day is damped by the diffusive heat flux into, or out of, the surface. In the zero layer model, which assumes a linear temperature profile throughout the ice block, these diffusive heat fluxes are considerably underestimated.

If variations in $T_s$ throughout the day are incorrectly simulated there will be errors in the calculation of the outgoing infra-red and turbulent fluxes. (Also possibly the solar flux if the albedo is dependent on the surface conditions of the ice). These errors can, in turn, affect the equilibrium ice depths.

A high resolution model would be required to resolve the diurnal temperature wave. (Semtner's 3-level model may well not have sufficient resolution near to the ice surface). However, this problem is similar to that which has already been solved in the Met O 20 soil model by the use of a surface heat capacity term (Carson, 1980). In fact, providing the ice thickness is considerably greater than the e-folding depth of the diurnal temperature wave, the problem is identical to that in the soil model. If the ice is thin the surface heat capacity should be dependent on the ice thickness, although such sophistication cannot really be justified in the zero layer model (in which other important effects such as ice dynamics are not represented).

With such a term included the basic equations become (see Appendix B):

a. No surface melting

$$\kappa\frac{(\bar{T}_* - T_B)}{h} + C_*^{(d)}\frac{dT_*}{dt} = -R_{LU} + R_{LD} + (1-\alpha)R_S - H_S - H_L \qquad (4.1)$$

$$\frac{\kappa(\bar{T}_* - T_B)}{h} = -F_B - \rho\frac{dh_2}{dt} \qquad (4.2)$$

$$T(h_2, t) = T_B \qquad (4.3)$$

where $C_*^{(d)}$ is a surface heat capacity appropriate to diurnal timescales and $\bar{T}_*$ is the daily mean temperature.

b. Surface melting

When there is surface melting $T_*$ is fixed so that $\frac{dT_*}{dt} = 0$ and the heat capacity term does not contribute. The equations governing this regime are therefore

$$\frac{\kappa(\bar{T}_* - T_B)}{h} = -R_{LU} + R_{LD} + (1-\alpha)R_S - H_S - H_L - \rho\frac{dh_1}{dt} \qquad (4.4)$$

$$T(h_1, t) = T_0 \quad . \qquad (4.5)$$

Equations (4.2) and (4.3) are also applicable in this regime.

The $C_*^{(d)}$ in (4.1) is a surface heat capacity term which is chosen so that the diurnal range of surface temperature is simulated correctly. The $C_*^{(d)}\frac{dT_*}{dt}$ term acts to damp the surface temperature oscillations and essentially parametrises the damping effect of the depth dependent diurnal wave. Theoretical arguments

suggest that $C_*^{(d)}$ should be assigned the value $C_*^{(d)} = c\rho\delta/\sqrt{2}$ where $\delta = (\kappa\tau/\pi c\rho)^{1/2}$ is the e-folding depth introduced in the previous section (see Appendix B for details).

However, these arguments are based on a very simplified solution of the diffusion equation and this expression should be used only as a guide for the value of $C_*^{(d)}$ (see Appendix B for details). In practice $C_*^{(d)}$ should be tuned so that a realistic diurnal range of temperature is produced.

The temperature gradient terms in (4.1) to (4.5), arising from the linear profile, should not be evaluated with a diurnal cycle in $T_*$ since they are only applicable to the seasonal timescale. In applications reported later the daily mean temperature has been used in these terms. Also over seasonal timescales the $C_*^{(d)}\frac{dT_*}{dt}$ term should not contribute to the heat budget since $C_*^{(d)}$ has been chosen explicitly with the diurnal cycle in mind. In fact, this term is small for seasonal timescales. Quantitative estimates derived from experiments with the model will be given later.

With a surface heat capacity term included, the heat balance equation (see 2.10) becomes

$$C_*^{(d)}\frac{dT_*}{dt} = -R_{LU} + R_{LD} + (1-\alpha)R_S - H_S - H_L + F_B + q\frac{dh}{dt} \quad . \quad (4.6)$$

The linear part of the profile does not contribute in this equation.

It is worth making the final point that $C_*$ could be chosen for the seasonal timescale so that differences between the zero and multi-level models could be reduced without tuning the heat diffusivities. However, if this were done the diurnal cycle would be too heavily damped.

## 5. The dual timestep model

The equations used in the dual timestep model (without snow cover) are

$$\frac{\kappa(\bar{T}_* - T_B)}{h} + C_* \frac{\Delta T_*}{\Delta t} = -R_{LU} + R_{LD} + (1-\alpha)R_S - H_S - H_L \qquad (5.1)$$

and, from equation (2.11),

$$h(t) = h(t_0) - \frac{1}{q_v}\int_{t_0}^{t} \left\{ -R_{LU} + R_{LD} + (1-\alpha)R_S - H_S - H_L + F_B \right\} dt \,. \qquad (5.2)$$

The timestep used to update the ice depth $h(t)$ is taken to be considerably longer (typically 1 to 5 days) than the timestep used in the solution of the surface balance equation. (Typically $\Delta t \lesssim 1$ hour). For melting or freezing occurring at the ice bottom the use of a longer timestep in the updating of the ice depth can be justified by the results of the previous sections. However, since surface melting occurs when the temperature predicted by (5.1) exceeds the melting point, the onset and cessation of surface melting may be incorrectly predicted when a longer timestep is used in the ice depth calculation. Errors due to the longer ice depth timestep will be assessed later by looking at the sensitivity of model results to the timesteps used.

Comparing (5.2) with (2.11) it will be noticed that the heat capacity term has been dropped in the dual timestep model. This is justified since over timescales of a day or more it is considerably smaller than the other terms in (5.2) (see Section 7). In coupled experiments this simplification will make the heat budget easier to interpret since the net heat input into the ice over a given period will be equal to the latent heat release due to ice depth change. In such experiments it is anticipated that the surface balance equation (5.1) will be solved every timestep (i.e. every 10-20 minutes), whereas the ice depth will be updated only when the ocean model is called.

## 6. Snow-covered ice

When the depth of a snow cover has to be monitored in addition to the ice depth, it becomes necessary to distinguish between changes at the upper and at the lower boundary.

An additional coordinate, $h_3$, is now required, as defined in Fig. 2. The snow depth, $h_s$ is given by

$$h_s = h_1 - h_3 \tag{6.1}$$

and, as before, the ice depth, $h$, is

$$h = h_2 - h_1 \quad . \tag{6.2}$$

Assuming a linear temperature gradient through the combined snow-ice layer eqns. (4.1) - (4.3), which apply when there is no surface melting, become:

$$\frac{\kappa(\bar{T}_* - T_B)}{h + \kappa/\kappa_s \cdot h_s} + C_*^{(d)} \frac{d\bar{T}_*}{dt} = -R_{LU} + R_{LD} + (1-\alpha_s)R_s - H_s - H_L \qquad (6.3)$$

$$\frac{\kappa(\bar{T}_* - T_B)}{h + \kappa/\kappa_s \cdot h_s} = -F_B - q_l \frac{dh_2}{dt} \qquad (6.4)$$

$$T(h_2, t) = T_B \quad . \qquad (6.5)$$

In addition, we have

$$\frac{dh_3}{dt} = - \text{ snowfall} . \qquad (6.6)$$

Equations (4.4) - (4.5), which apply when there is surface melting, become:

$$\frac{\kappa(\bar{T}_* - T_B)}{h + \kappa/\kappa_s \cdot h_s} = -R_{LU} + R_{LD} + (1-\alpha_s)R_s - H_s - H_L$$
$$- q_s \frac{dh_{3,melt}}{dt} \cdot S(h_s) - q_l \frac{dh_1}{dt}\left(1 - S(h_s)\right) \qquad (6.7)$$

$$\left.\begin{aligned} T(h_3, t) &= T_o^{(s)} \qquad \text{if } h_s > 0 \\ T(h_1, t) &= T_o \qquad \text{if } h_s = 0 \end{aligned}\right\} \qquad (6.8)$$

where $\frac{dh_{3,melt}}{dt}$ is the rate of change of $h_3$ due to snow melt, $T_o^{(s)}$ is the melting point of snow (usually taken as 273.15K), and $S$ is the step function defined by

$$S(h_s) = \begin{cases} 1 & \text{if } h_s > 0 \\ 0 & \text{if } h_s = 0 \end{cases} .$$

In addition,

$$\frac{dh_3}{dt} = \frac{dh_{3,melt}}{dt} - \text{Snowfall} \quad . \tag{6.9}$$

Note that eqns. (6.4) and (6.5) also apply when there is surface melting.

Dual timestep model

In the dual timestep model snow depth is updated with the same frequency as the ice depth. The equations used now depend on which melting regime operates.

a. No surface melting

By analogy with the snow-free case, we have:

$$\frac{\kappa(\bar{T}_* - T_B)}{h + \kappa/\kappa_s \cdot h_s} + C_* \frac{\Delta T_*}{\Delta t} = -R_{LU} + R_{LD} + (1-\alpha_s)R_s - H_s - H_L \tag{6.10}$$

and

$$h(t) = h(t_0) - \frac{1}{\rho_I} \int_{t_0}^{t} \left\{ -R_{LU} + R_{LD} + (1-\alpha_s)R_s - H_s - H_L + F_B \right\} dt \tag{6.11}$$

since changes in ice depth occur at only one boundary (the lower boundary) when the surface temperature is below freezing (and mass changes due to sublimation are neglected). However, changes in snow depth can occur at the upper boundary, due to snowfall i.e.

$$h_s(t) = h_s(t_0) + \int_{t_0}^{t} (\text{snowfall})\, dt \, . \tag{6.12}$$

b. Surface melting

Here the equations differ from the snow-free case because of the necessity to treat changes at the upper and at the lower boundary separately. Changes at the lower boundary are straightforward; from eqn. (6.4) we have:

$$h_2(t) = h_2(t_o) - \frac{1}{q_f}\int_{t_o}^{t}\left\{\frac{K(\bar{T}_* - T_B)}{h + K/K_s \cdot h_s} + F_B\right\} dt \quad . \tag{6.13}$$

At the upper snow boundary

$$h_3(t) = h_3(t_o) + \frac{1}{q_s}\int_{t_o}^{t}\left\{-R_w + R_{LD} + (1-\alpha_s)R_s - H_s - H_L - \frac{K(\bar{T}_* - T_B)}{h + K/K_s \cdot h_s}\right\} dt \tag{6.14}$$
$$- \int_{t_o}^{t} (\text{snowfall})\, dt \, .$$

Then if it is assumed that there is no ablation of ice from the upper boundary (only ablation of snow), eqns. (6.1) and (6.2) give:

$$h_s(t) = h_s(t_o) - h_3(t) + h_3(t_o) \tag{6.15}$$

and

$$h(t) = h(t_o) + h_2(t) - h_2(t_o) \quad . \tag{6.16}$$

However, if the snow depth predicted by eqn. (6.15) is negative, there is sufficient energy available in the period between $t_o$ and $t$ to remove the snow cover totally and to melt some of the underlying ice. A correction must then be made to the predicted ice depth (eqn. (6.16)) to allow for this i.e.

$$h(t) = h(t_o) + \left(h_2(t) - h_2(t_o)\right) + \frac{\rho_s}{\rho} . h_s(t)$$

where $h_2(t) - h_2(t_o)$ is given by eqn. (6.13) as before

and the snow depth then set to zero.

## 7. Tests of the dual timestep formulation

A number of experiments were carried out to test the effect of updating the snow and ice depths with a different timestep from that used to update the surface temperature. In each experiment the surface forcing contained both seasonal and diurnal variations. On the seasonal timescale Fletcher's fluxes as used by Semtner (1976), were used (see Table 1). To simulate the diurnal cycle the incoming short wave flux at the ice surface was assumed to be given by the expression

$$R_s(t;\tilde{t}) = Q(\tilde{t}) . \cos\left(Z(t;\tilde{t})\right) \qquad (7.1)$$

where $t$ and $\tilde{t}$ denote time coordinates representing diurnal and seasonal changes respectively. $Z(t,\tilde{t})$ is the zenith angle and $Q(\tilde{t})$ is chosen so that the mean short wave flux over a given day agrees with the value obtained for that day by interpolation of Fletcher's monthly mean values. The diurnal cycle was not included in the incoming longwave or

turbulent fluxes. The prescription given in (7.1) leads to a reasonable representation of the diurnal cycle in that the day length is correctly predicted as a function of latitude and time of year. (It can also deal with the permanent polar night and day). Further explanation of the method used to simulate the diurnal cycle can be found in Appendix C. The diurnal cycle used in the experiments described here was that given by (7.1) at 70N. This is illustrated in Fig. 6 for various times of year, assuming a daily mean of 100 Wm-2 throughout.

The albedo formulation used by Semtner (1976) involves a dependence on the depth of snow following the onset of surface melting (see Table 1). This affects the amount of net solar radiation available at the surface. Since the model is very sensitive to changes in the surface forcing (Bottomley, (1984)), it can be expected that this dependence of albedo on snow depth will make a significant contribution to differences between experiments with differing periods between snow and ice depth updates. Therefore, one set of experiments was carried out in which the depth dependence of the snow albedo was removed, and this was compared with another set in which Semtner's albedo formulation was used without modification. Each set comprises three experiments. In one, the control experiment, surface temperature and snow and ice depths are all updated every hour. In the other two, ice and snow depths are updated less frequently than surface temperature i.e. every 24 hours and every 5 days, compared with every hour for surface temperature.

In all experiments the snowfall was taken from Semtner (1976) and the model parameters were assigned the values given in Table 2. Following Semtner (1976) the bare ice albedo was enhanced to allow for

the effects of penetrative radiation. Integrations were made for 50 years, by which time equilibrium cycles of $T_*$, $h$ and $h_s$ had been established.

Equilibrium monthly mean values of surface temperature, ice and snow depth for the set of experiments in which the modified albedo formulation (i.e. no dependence on snow depth, see Table 1) was used, are shown in Tables 3-5. The equilibrium cycles for the control experiment are also shown in Fig. 7. Table 6 contains monthly mean values of the two terms on the left hand side of the surface balance equation (6.10) for this latter experiment. The contribution from the surface heat capacity term is considerably smaller than that arising from the linear gradient term, as would be expected over seasonal timescales. It is therefore reasonable to neglect the heat capacity term in the ice and snow depth calculations, as described in Section 5.

The seasonal variation in both the surface temperature and the snow depth is not significantly affected by reducing the frequency with which the ice and snow depths are updated. In general the discrepancy between the monthly mean values of $T_*$ for the 1 hour and the 5 day update is less than 0.06K, which corresponds roughly to $\approx$ 0.2 Wm-2. Although the discrepancy is substantially higher in September ($\sim$ 0.5K), the monthly mean values here are distorted by differences in the period for which the ice is effectively snow-free i.e. in the period during which the low, bare-ice albedo is in force.

The mean ice depth increases as the length of time between ice and snow depth updates is increased. The greatest differences in monthly mean ice depths are observed during the melting season when the most rapid changes in ice depth occur and, therefore, the frequency with

which the ice depth is updated is expected to be most significant. The maximum differences between the monthly mean ice depths for the 1 hour and the 24 hour update, and between those for the 1 hour and the 5 day update are 6 cms (July and August) and 17 cms (July), respectively. The maximum difference in monthly mean snow depth is only 2 cms.

Equilibrium annual mean ice depths for all three experiments are compared in Table 7 with those obtained in the corresponding experiments using the unmodified Semtner albedo formulation i.e. the experiments in which the albedo value decreases as the depth of the snow cover decreases during the melting season. Ice depths are lower in the latter set of experiments than in their counterparts because of this reduced albedo. As expected, the results for the 24 hour and the 5 day ice and snow depth updates diverge more strongly from those for the control experiment than in the experiments in which the albedo is not snow depth dependent. The rapid changes in snow depth and thereby in albedo - which occur during the melting season can be followed if a 1 hour, or even a 24 hour timestep, is used (see Fig. 8). However, if the snow depth is updated only every 5 days, these changes are not resolved and the change of albedo formulation has little effect.

It should be noted that these experiments are relevant for situations in which there is a perennial ice cover. Similar experiments were also carried out, with different atmospheric forcing, in which open water is periodically formed. In fact, multi-year equilibrium cycles of ice depth are established (similar to those reported by Semtner (1976)) which are sensitive to the timing of the transition between open water and ice in relation to the period of heavy snowfall which occurs in the autumn in Semtner's snowfall formulation. Therefore the effect of

varying the frequency with which the ice depth is updated is enhanced since, in general, this changes the timing of the transition. In equivalent experiments, but with zero snowfall, multi-year cycles are not set up and differences in equilibrium annual mean ice depth are small: for $\Delta t$ = 1 hour, 1 day and 5 days the mean ice depths are 0.81 m, 0.82 m and 0.80 m respectively.

## 8. Summary and Discussion

The physical basis of a scheme in which the surface temperature of sea-ice is updated every atmospheric model timestep (i.e. every 10-20 mins.) along with the land and land-ice surface temperatures, but the ice depth is only updated every N days has been investigated.

Changes in ice depth can occur both at the upper and at the lower boundary of the ice block. Solution of the temperature diffusion equation shows that, for thick ice ($\gtrsim$ 2m), changes in surface temperature occurring on diurnal or synoptic timescales are not propagated to the bottom of the ice. The effects of changes occurring on the seasonal timescale, however, are felt throughout the block. Therefore, for ice of thickness a metre or more only the longer timescale components of the variation in surface temperature affects the changes in ice depth at the lower boundary. At the upper boundary though, changes can occur in response to variations in surface forcing on all timescales, including the diurnal.

Observations in perennial sea-ice indicate that on seasonal timescales the temperature profile within the ice is linear for most of the year. The exceptions occur during spring and autumn when the variations in surface temperature are most rapid. If a linear

temperature profile is assumed during these periods also, a net excess of energy is made available for ice ablation, resulting in equilibrium ice depths which are lower than observed.

However the assumption of a linear temperature profile in thick ice is not applicable to the diurnal timescale i.e. the timescale on which the surface temperature is to be updated. In reality the temperature gradient (and therefore the diffusive heat flux) at the surface of the ice is much greater than that implied by a linear profile. Therefore, since the diffusive heat flux acts to damp the variations in surface temperature, the assumption of a linear change in temperature between the surface and the lower boundary results in an overestimation of the diurnal range of surface temperature. However the diurnal range can be simulated correctly by the introduction of an additional diffusive term $C_*^{(d)} \frac{dT_*}{dt}$ into the surface balance equation, where $C_*^{(d)}$ is a surface heat capacity appropriate for diurnal or synoptic timescales.

Maykut (1978) suggests that the temperature profile in rapidly growing young ice is always approximately linear because it responds quickly to surface temperature changes. It may be, then, that for thin ice a linear profile is a reasonable approximation on all timescales.

In the dual timestep scheme proposed here the ice and snow depth is updated every few days only so that the variations in ice depth which would otherwise occur due to the diurnal cycle of surface temperature are not resolved. However experiments with the model have shown that for perennial sea-ice this does not have a very significant effect on the equilibrium annual mean ice depth. It should be noted, though, that

the magnitude of the effect is increased if a depth dependent albedo formulation is used. Some retuning of the model parameters might be necessary in this case.

References


Bottomley, M. 1984 The response of a simple thermodynamic sea-ice model to GCM forcing for perennial sea-ice.
Met O 20 Tech. Note (in preparation).

Bryan, K. 1969 Climate and the ocean circulation III. The ocean model.
Mon. Weath. Rev., 97 (11), 806.

Carson, D.J. 1980 Current parametrisations of land-surface processes in atmospheric general circulation models.
Met O 20 Tech. Note No. II/152.

Maykut, G.A. 1978 Energy exchange over young sea-ice in the central Arctic.
J. Geophys. Res. 83, (C7), 3646.

Maykut, G.A. and Untersteiner, N. 1971 Some results from a time-dependent thermodynamic model of sea-ice.
J. Geophys. Res., 76 (C6), 1550.

Parkinson, C.L. and Washington, W.M. 1979 A large-scale numerical model of sea-ice.
J. Geophys. Res., 84 (C1), 311.

Sellers, W.D. 1965 Physical Climatology, The University of Chicago Press, Chicago and London.

Semtner, A.J. Jr., 1976 A model for the thermodynamic growth of sea-ice in numerical investigations of climate.
J. Phys. Oceanogr., 6, 379.

## Appendix A List of Symbols

| | |
|---|---|
| $A(z)$ | Amplitude of temperature wave at depth z. |
| $c$ | Specific heat capacity of ice. |
| $c_*^{(d)}$ | Surface heat capacity appropriate for diurnal timescales. |
| $F_B$ | Upward heat flux from the ocean into the ice. |
| $h, h_s$ | Ice depth and snow depth respectively. |
| $H$ | Heat content of snow-ice block. |
| $H_s$ | Sensible heat flux. |
| $H_L$ | Latent heat flux. |
| $q, q_s$ | Latent heats of fusion of ice and snow respectively. |
| $R_{LD}$ | Incoming long-wave radiation at surface. |
| $R_{LU}$ | Outgoing long-wave radiation at surface. |
| $R_s$ | Incoming short-wave radiation at surface. |
| $S(h)$ | Step function defined by $S(h_s) = 1$ if $h_s > 0$ <br> $= 0$ if $h_s = 0$ |
| $t$ | Time. |
| $T$ | Temperature. |
| $T_*$ | Surface temperature. |
| $\overline{T}_*$ | Daily mean surface temperature. |
| $T_B$ | Temperature at bottom of ice. |
| $T_o$ | Surface melting point temperature. |
| $z$ | Vertical coordinate, defined to be positive downward. |
| $\alpha, \alpha_s$ | Surface albedo for ice and snow, respectively. |
| $\delta$ | Temperature wave e-folding depth. |
| $\kappa, \kappa_s$ | Thermal conductivity of ice and snow, respectively. |
| $\rho$ | Density of sea-ice. |

$\tau$ Timescale of temperature wave.

$\phi(z)$ Phase of temperature wave at depth .

$\omega$ Angular frequency of temperature wave.

## Appendix B The surface heat capacity

In this appendix the surface heat capacity term will be discussed in greater detail. Consider an ice block of thickness $h$. The temperature profile in the block is found by solving the diffusion equation

$$c\rho \frac{\partial T}{\partial t} = \frac{\partial}{\partial z}\left(\kappa \frac{\partial T}{\partial z}\right) \quad . \tag{B1}$$

Rather than actually solving (B1) it is useful to consider the vertically integrated equation i.e.

$$c\rho \int_{h_1}^{h_2} \frac{\partial T}{\partial t}.dz = \kappa \frac{\partial T}{\partial z}\bigg|_{h_2} - \kappa \frac{\partial T}{\partial z}\bigg|_{h_1} \quad . \tag{B2}$$

The surface heat capacity is defined by

$$c\rho \int_{h_1}^{h_2} \frac{\partial T}{\partial t}.dz = \tilde{C}_*(t) \frac{dT_*}{dt} \quad . \tag{B2}$$

In order to reduce (B2) to a balance equation involving only $T_*$ it is necessary to replace $\tilde{C}_*(t)$ by a typical constant value $C_*$. For diurnal variations in surface temperature there will be no corresponding signal in the bottom diffusive heat flux $-\kappa \frac{\partial T}{\partial z}\Big|_{h_2}$. It is therefore possible to write

$$-\kappa \frac{\partial T}{\partial z}\bigg|_{h_1}^{(\text{diurnal})} = C_*^{(d)} \frac{dT_*}{dt} \quad . \tag{B4}$$

$C_*^{(L)}$ can be determined by comparing the solution of the surface balance equation using simple forcing with the solution obtained by explicit integration of the diffusion equation. It can be shown that the diurnal range of temperature will be the same provided

$$C_* \approx \frac{1}{\sqrt{2}} c\rho\delta \qquad \text{(B5)}$$

where $\delta = \left(\frac{k\tau}{\pi c\rho}\right)^{1/2}$, with $\tau$ = 24 hours, is the e-folding depth of the diurnal temperature wave. The exact form of $C_*$ is actually dependent upon the ice thickness $h$ although, provided $h \gg \delta$, the result (B5) is a very good approximation.

## Appendix C Treatment of the diurnal cycle

At the top of the atmosphere the incoming solar radiation is given by

$$S_{TOP}(t) = S_0 \left( \frac{\bar{d}}{d(t)} \right)^2 \cos Z(t) \qquad (C1)$$

where $Z$ is the zenith angle which depends on the latitude, time of year and time of day (Sellers, 1965). $S_0$ is the solar constant ($S_0 \approx 1376$ Wm-2) and $d$ is the distance of the earth from the sun ($\bar{d}$ is the annual mean distance). Equation (C1) can be written out explicitly as

$$S_{TOP}(t) = S_0 \left( \frac{\bar{d}}{d(t)} \right)^2 \left( \sin\phi . \sin\delta + \cos\phi . \cos\delta . \cos\left( \frac{2\pi}{T} t \right) \right) \qquad (C2)$$

where $\phi$ is the latitude, $\delta$ is the solar declination (angular distance north of the equator) and $\left(\frac{2\pi}{T}\right)t$ is the hour angle ($T$ = 24 hours). (Sellers, 1965)

In order to represent the solar heating at the surface a formula similar to (C2) is assumed to apply. At the surface the incoming solar flux is taken to be

$$R_s(t;\tilde{t}) = Q(\tilde{t}) \left( \sin\phi . \sin\delta(\tilde{t}) + \cos\phi . \cos\delta(\tilde{t}) . \cos\left( \frac{2\pi}{T} t \right) \right) \qquad (C3)$$

In (C3) the time coordinate $\tilde{t}$ changes with the time of year and $t$ with the time of day. $Q(\tilde{t})$ in (C3) is chosen so that the daily mean value of $R_s(t,\tilde{t})$ agrees with climatological estimates i.e. if $H$ is the half day length (and therefore $2H$ is the total period of daylight) then

$$\bar{R}_s(\tilde{t}) = \frac{1}{T}\int_{-H}^{+H} R_s(t;\tilde{t})\,dt \quad . \qquad (C4)$$

From (C3) and (C4) it is easily shown that

$$Q(\tilde{t}) = \frac{\pi}{2}\bar{R}_s(\tilde{t})\left\{\frac{\pi H}{T}\sin\phi.\sin\delta + \frac{1}{2}\cos\phi.\cos\delta.\sin\left(\frac{2\pi}{T}H\right)\right\}^{-1} \qquad (C5)$$

The half day length $(H)$ appearing in (C5) is determined from the relation (Sellers, 1965)

$$\cos H = -\tan\phi.\tan\delta \quad . \qquad (C6)$$

To summarise:

i. The daily mean incoming short wave radiation at the surface (i.e. $\bar{S}(\tilde{t})$) is determined by interpolation of Fletcher's monthly mean values.

ii. Equation (C5) is then used to find the appropriate $Q(\tilde{t})$ for that day using the half day length given by (C6).

iii. Equation (C3) is used to calculate the diurnal cycle in surface net short wave radiation throughout the day.

More accurate empirical formulae (Parkinson and Washington, 1979) can be used to estimate the diurnal cycle, although since (C3) ensures that the daily mean radiation, as well as the day length, is correctly determined the above treatment was felt to be adequate for the studies discussed in this note.

| | J | F | M | A | M | J | J | A | S | O | N | D |
|---|---|---|---|---|---|---|---|---|---|---|---|---|
| Incoming short-wave radiation, $R_S$ ($Jm^{-2}$) | 0 | 0 | 30.7 | 159.9 | 285.8 | 310.0 | 219.6 | 145.3 | 59.7 | 6.4 | 0 | 0 |
| Incoming long-wave radiation, $R_{LD}$ ($Jm^{-2}$) | 167.9 | 166.3 | 166.3 | 187.3 | 243.8 | 290.6 | 308.4 | 302.0 | 266.4 | 224.4 | 180.8 | 176.0 |
| Sensible heat flux, $H_S$ ($Jm^{-2}$) | 19.05 | 12.27 | 11.63 | 4.68 | -7.27 | -6.30 | -4.84 | -6.46 | -2.74 | 1.61 | 9.04 | 12.76 |
| Latent heat flux, $H_L$ ($Jm^{-2}$) | 0 | -0.32 | -0.48 | -1.45 | -7.43 | -11.30 | -10.33 | -10.66 | -6.30 | -3.07 | -0.16 | -0.16 |
| Surface albedo*, $\alpha$ | - | - | 0.83 | 0.81 | 0.82 | 0.78 | 0.64 | 0.69 | 0.84 | 0.85 | - | - |

Table 1: Mean monthly values of forcing fluxes and surface albedo.

*Semtner (1976) assumes that the albedo of snow decreases linearly with snow thickness from the value at the onset of melting to that of bare ice at the end of melting.

This dependence of albedo on snow depth was retained in one of the sets of experiments reported here, but neglected in the other.

| | |
|---|---|
| $K$ | 2.166 Jm-1K-1S-1 |
| $K_s$ | 0.3299 Jm-1K-1S-1 |
| $C_*^{(d)}$ | 2.26 x 105 Jm-2K-1 |
| $F_B$ | 2.0 Wm-2 |
| $q_v$ | 3.014 x 108 Jm-3 |
| $q_s$ | 1.097 x 108 Jm-3 |

Table 2: Model Parameters.

| Frequency of ice/snow depth update | Monthly Mean Surface Temperature (K) 1 hour | 24 hours | 5 days |
|---|---|---|---|
| Jan | 244.63 | 244.62 | 244.59 |
| Feb | 242.82 | 242.80 | 242.77 |
| March | 243.74 | 243.72 | 243.70 |
| April | 253.00 | 252.99 | 252.97 |
| May | 265.65 | 265.65 | 265.64 |
| June | 272.40 | 272.39 | 272.39 |
| July | 272.89 | 272.89 | 272.89 |
| Aug | 271.85 | 271.87 | 271.88 |
| Sept | 264.08 | 264.08 | 264.53 |
| Oct | 254.50 | 254.49 | 254.53 |
| Nov | 246.54 | 246.52 | 246.50 |
| Dec | 245.33 | 245.31 | 245.28 |

Table 3: Equilibrium monthly mean surface temperature for various frequencies of ice and snow depth update.

| Frequency of ice/snow depth update | Monthly Mean Snow Depth (M) 1 hour | 24 hours | 5 days |
|---|---|---|---|
| Jan | 0.28 | 0.28 | 0.27 |
| Feb | 0.29 | 0.29 | 0.28 |
| March | 0.30 | 0.29 | 0.29 |
| April | 0.31 | 0.30 | 0.30 |
| May | 0.34 | 0.33 | 0.32 |
| June | 0.12 | 0.12 | 0.14 |
| July | 0.00 | 0.00 | 0.00 |
| Aug | 0.00 | 0.00 | 0.00 |
| Sept | 0.07 | 0.07 | 0.05 |
| Oct | 0.20 | 0.19 | 0.18 |
| Nov | 0.27 | 0.26 | 0.25 |
| Dec | 0.27 | 0.27 | 0.26 |

Table 4: Equilibrium monthly mean snow depth for various frequencies of ice and snow depth update.

| Frequency of ice/snow depth update | Monthly Mean Ice Depth (M) 1 hour | 24 hours | 5 days |
|---|---|---|---|
| Jan | 1.59 | 1.63 | 1.70 |
| Feb | 1.71 | 1.76 | 1.83 |
| March | 1.84 | 1.89 | 1.95 |
| April | 1.93 | 1.98 | 2.04 |
| May | 1.96 | 2.01 | 2.08 |
| June | 1.91 | 1.96 | 2.05 |
| July | 1.48 | 1.54 | 1.65 |
| Aug | 1.14 | 1.20 | 1.29 |
| Sept | 1.11 | 1.16 | 1.23 |
| Oct | 1.20 | 1.25 | 1.32 |
| Nov | 1.32 | 1.37 | 1.44 |
| Dec | 1.46 | 1.51 | 1.57 |

Table 5: Equilibrium monthly mean ice depth for various frequencies of ice and snow depth update.

| | $C_* \frac{\Delta T_*}{\Delta t}$ (Wm-2) | $\frac{K(\bar{T}_* - T_*)}{(h + K/K_e \cdot h_s)}$ (Wm-2) |
|---|---|---|
| Jan | -0.14 | -16.67 |
| Feb | -0.01 | -17.01 |
| March | 0.26 | -15.74 |
| April | 1.08 | -10.24 |
| May | 0.95 | -3.12 |
| June | 0.25 | 1.15 |
| July | -0.06 | 2.52 |
| Aug | -0.19 | 1.36 |
| Sept | -0.91 | -8.80 |
| Oct | -0.86 | -13.89 |
| Nov | -0.38 | -17.24 |
| Dec | 0.00 | -17.24 |

Table 6: Comparison of the contributions to the surface balance equation from the surface heat capacity term and the linear diffusive heat flux.
Values shown are monthly means at equilibrium.

| Frequency of ice/ snow depth update | Annual Mean Ice Depth (M) 1 hour | 24 hours | 5 days |
|---|---|---|---|
| Albedo not snow depth dependent | 1.55 | 1.60 | 1.68 |
| Albedo dependent on snow depth after onset of melting | 1.38 | 1.47 | 1.63 |

Table 7: Equilibrium annual mean ice depth for various frequencies of ice and snow depth update and two different albedo formulations.

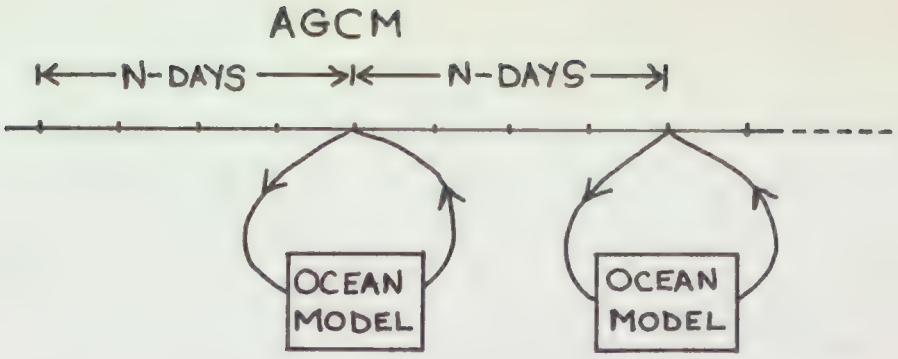


FIG. 1 : Typical mode of coupling.

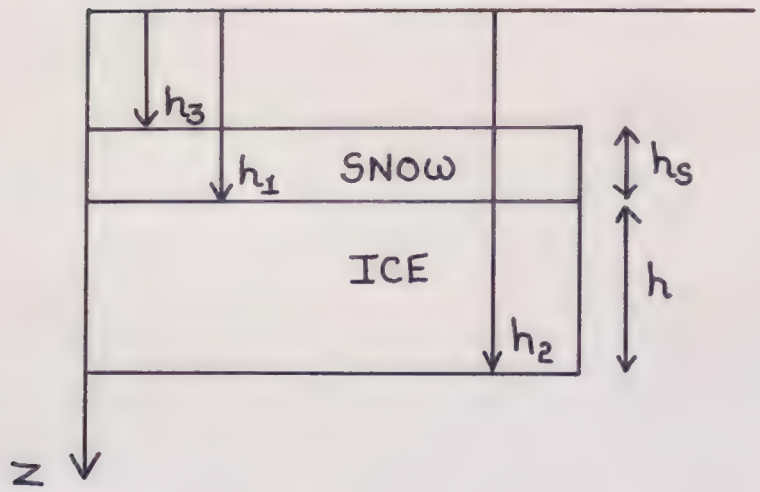


FIG. 2 : Definition of the coordinates $h_1$, $h_2$, $h_3$
$h_1$ is the distance from the origin of the upper boundary of the ice; $h_2$ and $h_3$ are the corresponding distances for the lower ice boundary and the upper boundary of the snow respectively.

The ice depth, h, is given by $h = h_2 - h_1$
and the snow depth by $h_s = h_1 - h_3$

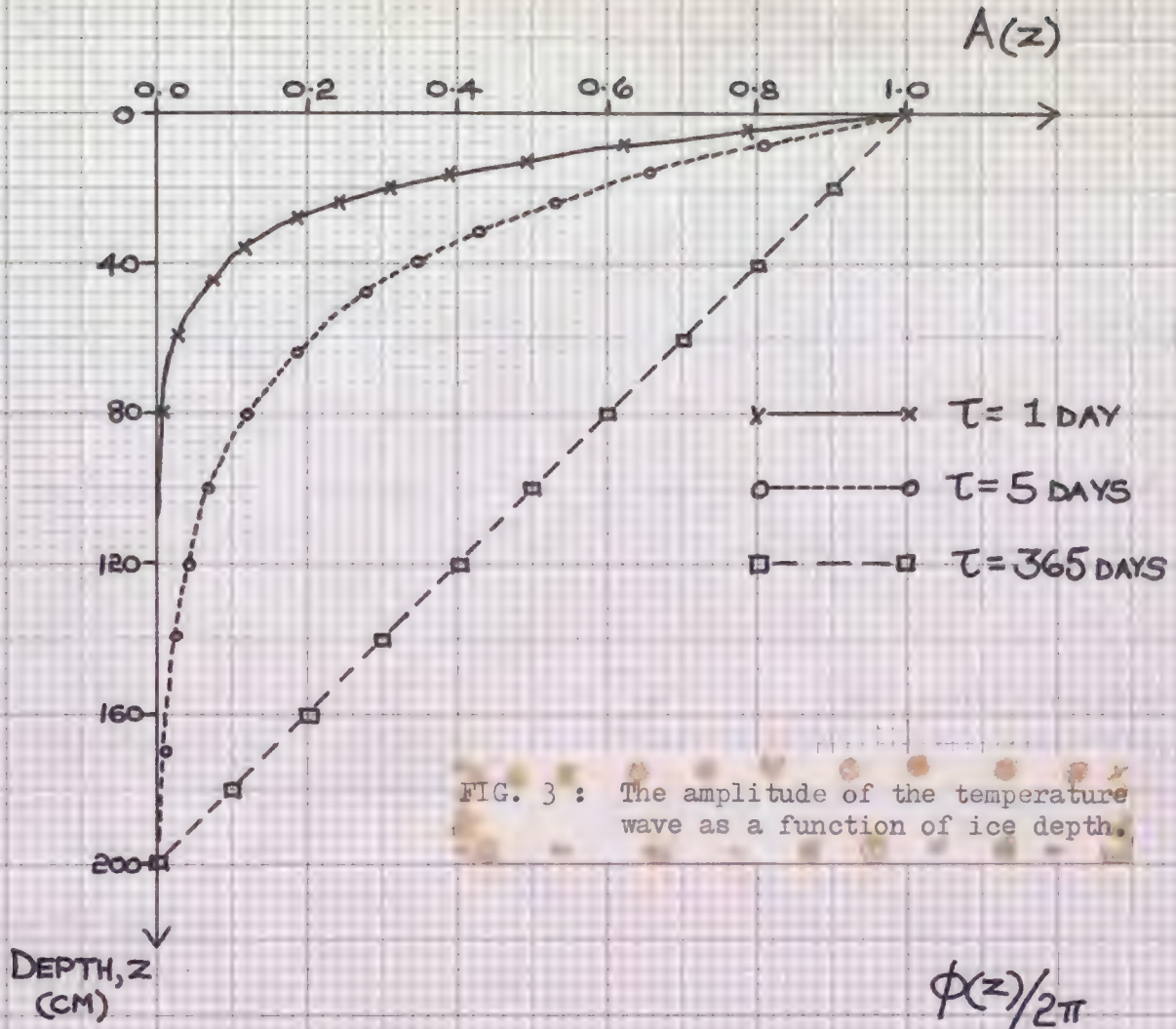


FIG. 3 : The amplitude of the temperature wave as a function of ice depth.

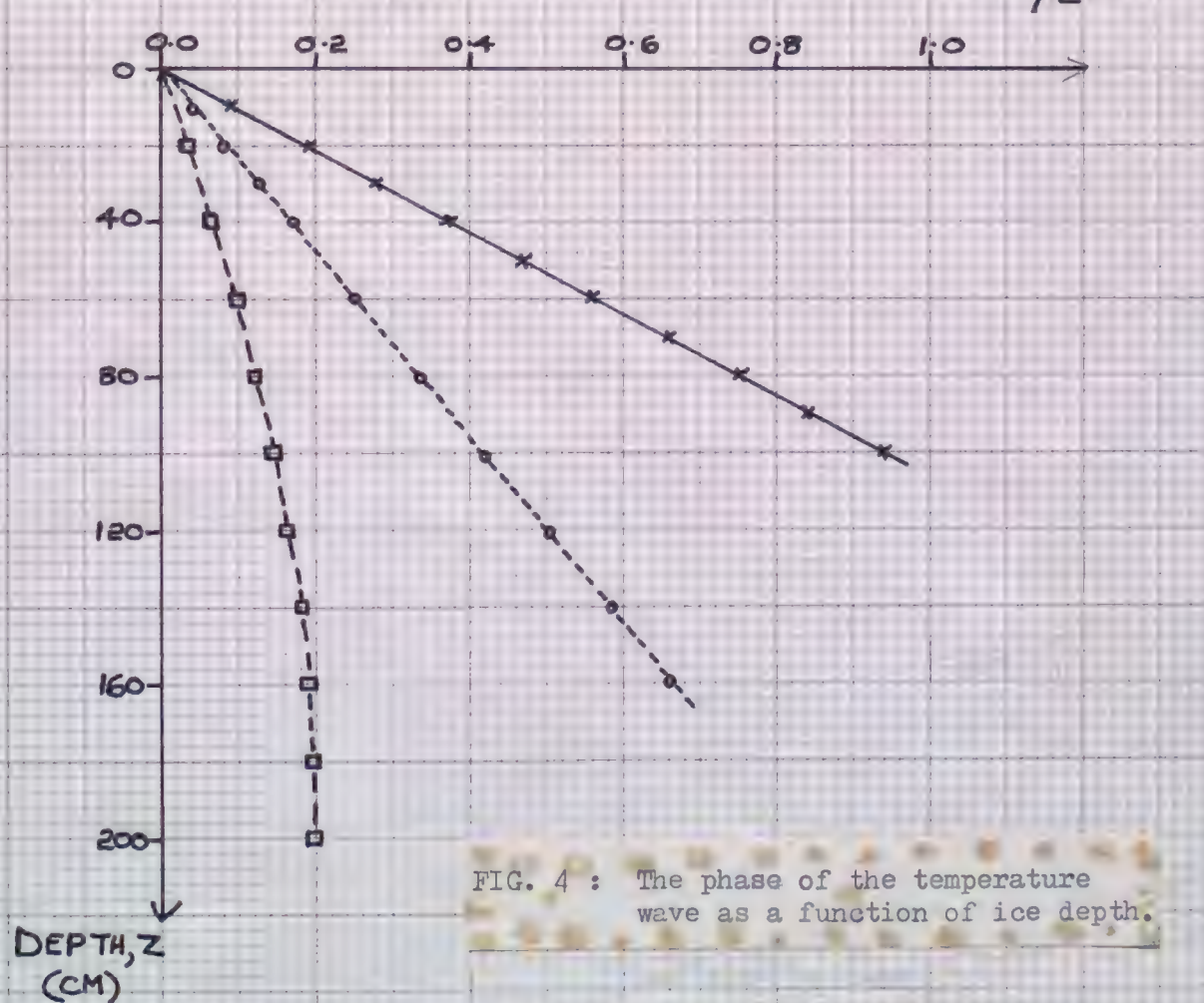


FIG. 4 : The phase of the temperature wave as a function of ice depth.

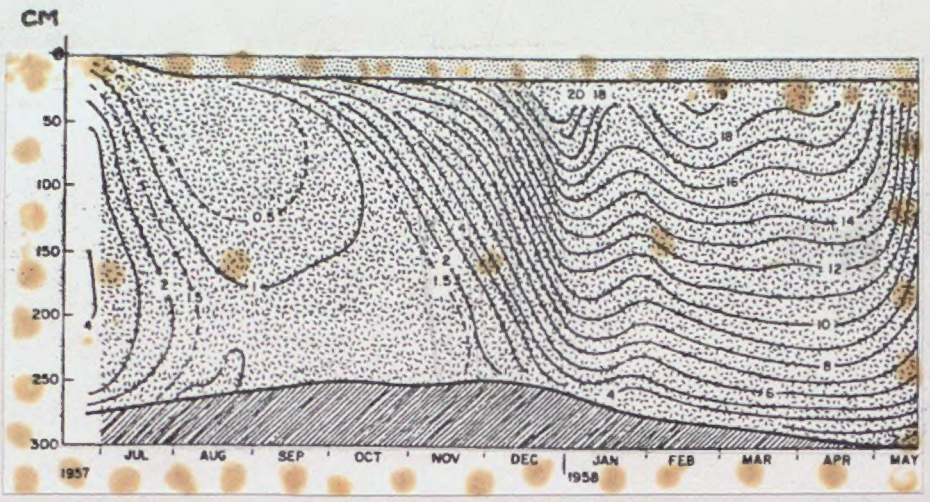


FIG. 5 : Observed temperature and thickness pattern of perennial sea-ice at IGY station alpha, 1957-1958. Isotherms are labelled in negative degrees Celsius. (Taken from Maykut and Untersteiner (1971)).

FIG. 6 : The diurnal cycle of solar radiation at 70N assuming a daily mean of 100 $W.m^{-2}$.

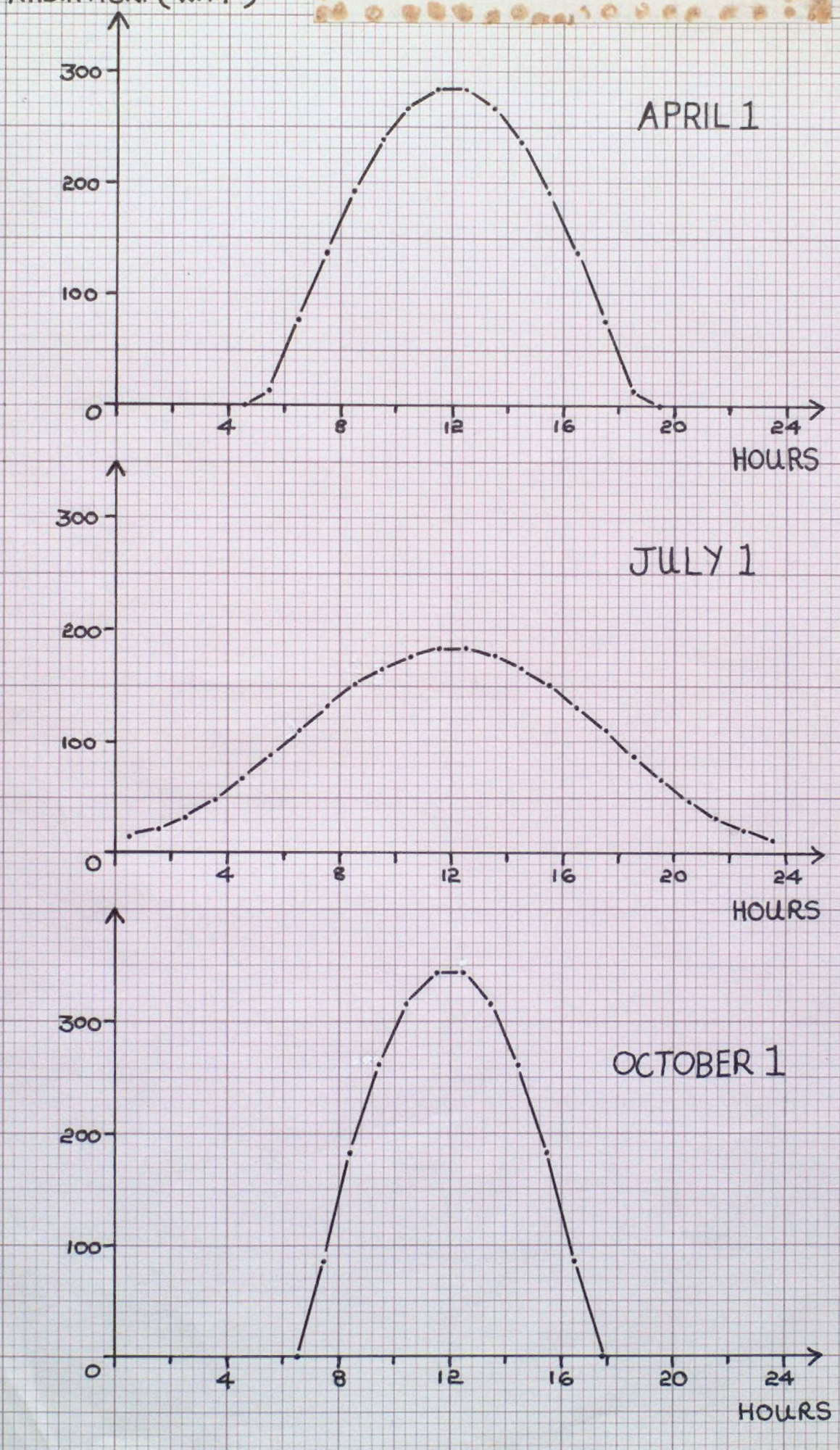

FIG. 7 : Equilibrium cycles of surface temperature and ice depth from the control experiment. Snow cover is indicated.

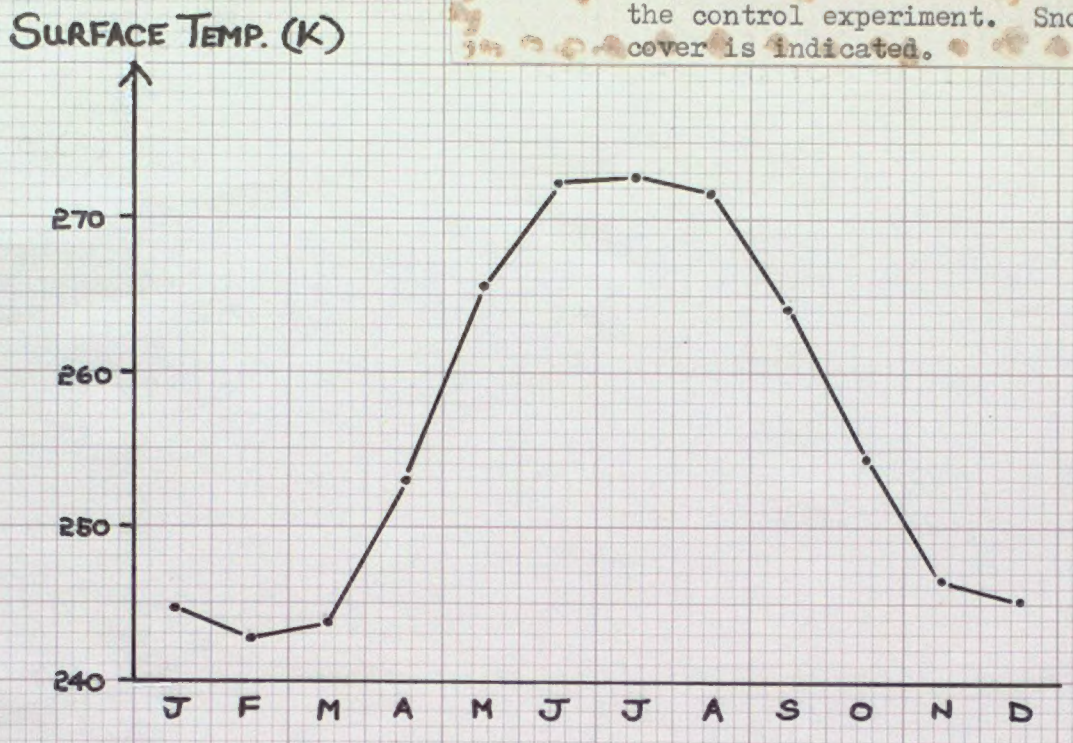


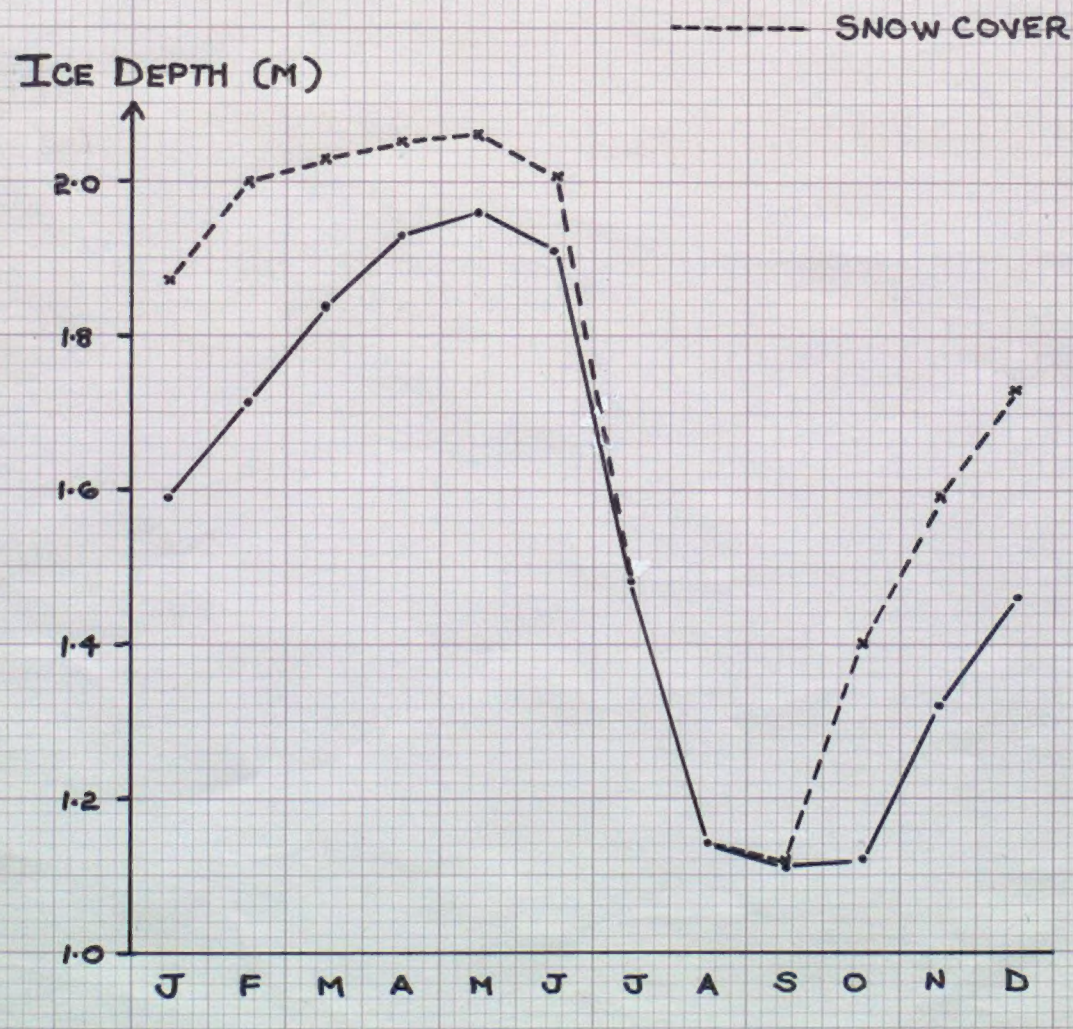

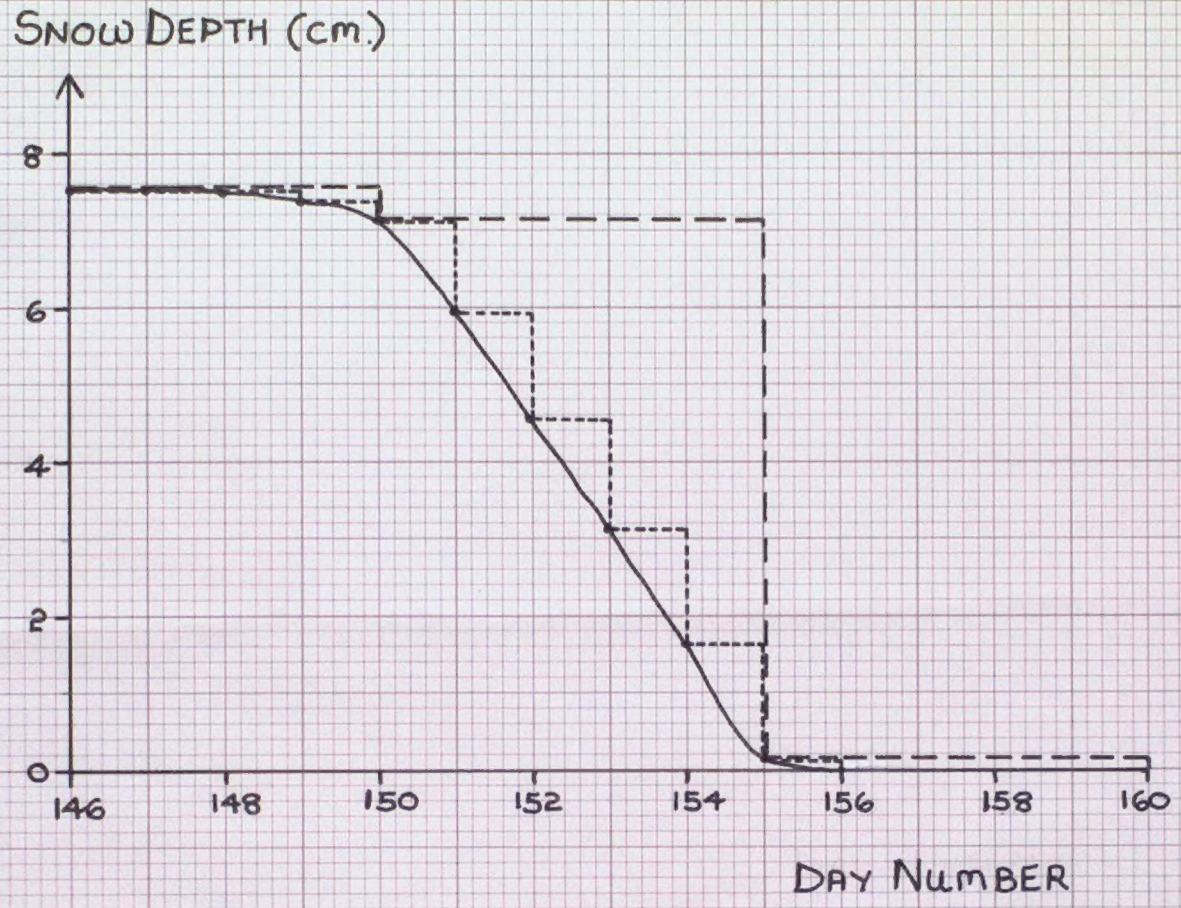


FIG. 8 : The change in snow depth during the melting season as determined using a 1 hour timestep (solid line). The broken lines show the corresponding change when the snow depth is updated every day (----------) and every 5 days (— — — —).